

# ANALYSIS OF REMAINING RISK OF LANDSLIDES IN NEPAL

Alessandra Mayumi NAKATA<sup>1</sup>, Hikaru TOMITA<sup>2</sup>, Masataka SHIGA<sup>3</sup>, Kazuo KONAGAI<sup>4</sup>, Takaaki Ikeda<sup>5</sup>, and Rama Mohan Pokhrel<sup>6</sup>

<sup>1</sup> Former Researcher, Institute of Urban Innovation, Yokohama National University  
(Tokiwadai 79-1, Hodogaya-ku, Yokohama 240-8501, Japan)  
E-mail: amnakata@gmail.com

<sup>2</sup> Former Graduate student, Graduate school of Urban Innovation, Yokohama National University  
(Tokiwadai 79-5, Hodogaya-ku, Yokohama 240-8501, Japan)  
E-mail: tomita-hikaru-vg@ynu.jp

<sup>3</sup> Ph.D Student, Department of Civil Engineering, Graduate school of Engineering, University of Tokyo (Komaba  
4-6-1, Meguro-ku, Tokyo, 153-8505 Japan)  
E-mail: shiga815@iis.u-tokyo.ac.jp

<sup>4</sup> Ph D., Principal Researcher, International Consortium on Landslides  
(Tanakaasukai-cho 138-1, Sakyo-ku, Kyoto, 606-8226, Japan)  
E-mail: kaz3776k@gmail.com

<sup>5</sup> Professor, Department of Civil and Environmental Engineering, Nagaoka University of Technology  
(1603-1, Kami-Tomioka-machi, Nagaoka-shi, Niigata, 940-2188, Japan)  
E-mail: ikeda@vos.nagaokaut.ac.jp

<sup>6</sup> Ph.D., Senior Research Associate, Department of Civil Engineering, University of Bristol, UK  
(Queens Building Room No.2, University walk, Bristol, BS8 1TR, UK)  
E-mail: r.pokhrel@bristol.ac.uk

We adopt a depth-integrated particle method as a primary analysis of the remaining risk of landslides in Dhunche and Ramche areas, Nepal, which was ravaged by the April 25, 2015 Gorkha Earthquake. Considering the difficulty in obtaining material properties of colluvium accumulated along gulleys on valley walls, the number of material parameters used in this evaluation procedure is limited as small as possible; the initial failure slope angle,  $i_f$ , Manning coefficient,  $n$ , for the flowing soil-water mixture, the angle of repose,  $i_d$ , at which the soil-water mixture on its depositional area stops spreading, and the rain concentration, RC, an index to describe rain-water collectivity of gulleys. We applied the procedure to our target area (3.5km by 2.62km) along the canyon of Trishuli River, Nepal. The result from this study indicates that colluvium soils remaining on 40-degree slopes or steeper are in the critical equilibrium, and can be detached at any time. However, even colluvium soils on gentler slopes such as the one in Ramche shows a creeping movement, and we need to keep a vigilant eye on these slopes.

**Key Words :** landslide, depth-integrated particle method, GPS, microtremor, simulation, Nepal

## 1. INTRODUCTION

The 2015 Nepal Earthquake (Mw = 7.8), also called the Gorkha Earthquake, was the worst natural disaster to strike Nepal since the 1934 Nepal–Bihar Earthquake. Both the debris masses that have already fallen into major rivers and unstable debris masses still perching atop of exposed bare slopes will cause long-lasting problems. This paper attempts to provide important parameters for identifying and estimating

the risk associated with the slope failures based on the evidence currently available in the mountains of Nepal. The procedure used herein is based on the idea developed by Nakata and Matsushima<sup>1,2)</sup> for widespread landslide-prone areas where a straightforward method of analyzing every detail of slope movement is unrealistic for perceiving the whole picture of the risk. The authors used the depth-integrated particle method (DIPM)<sup>2,3)</sup> to describe movements of all landslide masses within the target

area (3.5 km by 2.62 km) along the Trishuli River near Dhunche, one of the areas hardest hit by the earthquake. Three best-fitting parameters that describe landslide mass movements were obtained to minimize the distance to the perfect match,  $r$ . Then, we focused on the remaining debris masses that could have been detached during the earthquake and could be a residual risk to the communities and important facilities immediately below them.

Even slopes with their gradients less than the failure slope angle  $i_f$  obtained for the target area may require a vigilant watch. A colluvium soil mass on a slope near Ramche village in Rasuwa district located about 4 to 5 km south of the target area is slowly creeping year by year. Since the mass has been dragging down one of important traffic arteries, Pasang Lhamu Highway, we have been monitoring the movement of the soil mass on a periodic basis using a dual-frequency GPS system. In the light of the observed creeping nature of the slope, immediate problems will also be discussed herein.

## 2. METHODOLOGY

Our procedure towards the analysis of the remaining landslide area contains several steps. A starting point is the acquisition of the satellite images. Using two photogrammetric images taken by PRISM sensor assembled in ALOS satellite<sup>4)</sup> and evaluating as stereo-pairs, it is possible to construct a Digital Surface Model (DSM) whose minimum grid size is 5.0m horizontally and 1.0m vertically. Although ALOS satellite finished operation on May 2011, the data during its operation cover the entire earth surface with the aforementioned grid size. Therefore, the following analyses are possible in principle in any region on the earth.

Second step deals with the flow simulation of detached soil mass. We adopt a depth-integrated particle method with a simple particle interaction model, which allows us to evaluate a landslide-induced damaged area in a wide region simulation with a low computational cost. It is based on the commonly-used shallow water equation as follows:

$$\begin{aligned} \frac{\partial v_x}{\partial t} + v_x \frac{\partial v_x}{\partial x} + v_y \frac{\partial v_x}{\partial y} &= g_x - \frac{1}{\rho} \frac{\partial p}{\partial x} - \frac{\tau_{bx}}{\rho h} \\ \frac{\partial v_y}{\partial t} + v_x \frac{\partial v_y}{\partial x} + v_y \frac{\partial v_y}{\partial y} &= g_y - \frac{1}{\rho} \frac{\partial p}{\partial y} - \frac{\tau_{by}}{\rho h} \end{aligned} \quad (1)$$

where  $t$  is time,  $x$  and  $y$  are two orthogonal coordinates making up the slip surface,  $v_x$  and  $v_y$  are  $x$  and  $y$  components of a depth-integrated flow velocity vector,  $h$  is the thickness of the debris mass,  $g_x$  and  $g_y$  are  $x$  and  $y$  components of gravitational acceleration along the slip surface,  $p$  is the hydraulic pressure,  $\rho$  is the density of the debris mass, and  $\tau_{bx}$  and  $\tau_{by}$  are  $x$  and  $y$  components of the basal shear

stress,  $\tau_b$ , respectively.  $\tau_b$  is given by the following relation:

$$\tau_{cr} = \rho g R_h i_d \quad (2)$$

$$\tau_b = (\tau_{cr} + \rho g R_h i) \frac{v}{\|v\|} = \rho g R_h (i_d + i) \frac{v}{\|v\|} \quad (3)$$

$$i = \frac{n^2}{R_h^{4/3}} \|v\|^2 \quad (\text{Manning equation}) \quad (4)$$

where  $R_h$  is the hydraulic radius, which is almost identical to the debris depth  $h$  for a widespread flowing mass, and  $n$  is the Gauckler–Manning coefficient used in the Manning formula that empirically relates the average velocity of a liquid flowing in an open channel with the linear hydraulic head loss, which can often be approximated by the channel bed slope  $i$  when the flow is shallow.

In the time-marching DIPM calculation scheme, a debris mass is described as a two-dimensional assemblage of discrete particles on a slope carrying Lagrangian parameters. The DIPM is thus similar to smoothed particle hydrodynamics<sup>5,6)</sup> in the sense that a time-marching calculation scheme is utilized. However, it can maintain the movement of a rapidly flowing debris mass in a more stable manner because each particle is assumed to interact only with its neighboring particles. Each particle retains its volume unchanged. Therefore, when its neighboring particles exert compressive/repulsive forces on this particle, its height increases, and its base area is decreased. When neighboring particles move apart, they are detached from each other and no traction force is induced. The repulsive force is linearly related with the hydraulic pressure  $p$  in Equation (1), which is given by the following relationship:

$$p = \begin{cases} -\rho g \frac{h_0}{d_0} \left( \frac{1 - \|d\|/d_0}{1 + \|d\|/d_0} \right) \frac{d}{\|d\|} & (\|d\| < d_0) \\ 0 & (\|d\| > d_0) \end{cases} \quad (5)$$

where  $h_0$  and  $d_0$  are the initial height and width of particle (debris column). The volume  $V$  of each particle is thus given by

$$V = h_0 d_0^2 \quad (6)$$

## 3. STUDY AREAS

A rectangular area of 3.5 km by 2.62 km along the Trishuli River near Dhunche was studied in consideration of the importance of hydropower facilities. Ramche (1.62 km by 1.3km) was also chosen because of the presence of the Pasang Lhamu Highway leading to China (Fig. 1). According to Dhital, 2015 both areas are considered to have the same geological formations. Fig. 2 shows the cumulative frequency of slope inclinations in the two areas; The average inclination of slopes in Ramche is about 10 degrees smaller than that in Dhunche, and yet

greater part of the colluvium covering the slope is moving inch by inch. Black arrows in Fig. 3 show one section of Pasang Lhamu Highway in Ramche, which was constructed in 2003 across the creeping colluvium soil mass. This section had been carried steadily down until it sagged too much to take the traffic of the highway, and its new road shown by white arrows was constructed where the old one was once constructed.

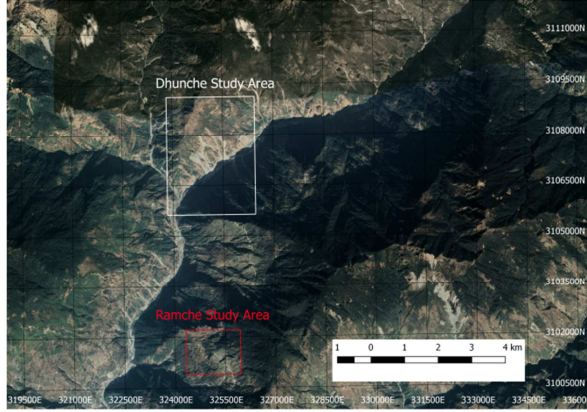


Fig. 1 Study areas location

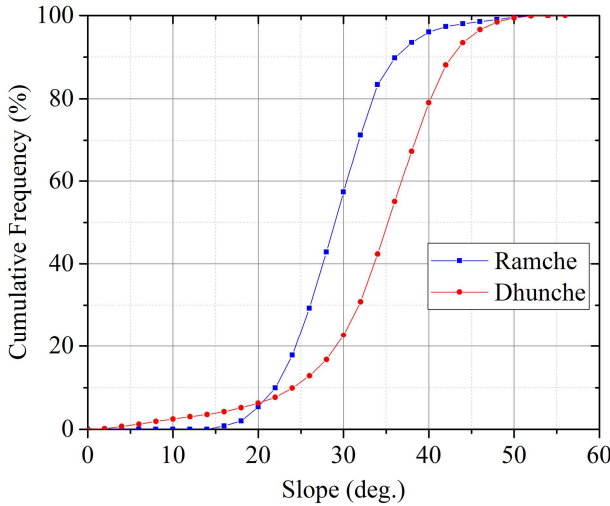


Fig. 2 Cumulative slope frequency in Ramche and Dhunche Village



Fig. 3 Former roads (Konagai et al., 2016)<sup>7)</sup>

## LANDSLIDE RISK

The Receiver operating characteristic (ROC) curve is drawn for the Dhunche area by plotting the true positive rate ( $TPR$  in Equation (8)) against the false positive rate ( $FPR$  in Equation (7)) at various sets of the three parameters,  $i_f$ ,  $n$ , and  $i_d$ , for a batch of landslide simulations. The closest point on the ROC curve to the upper-left corner represents the best set of the parameters, in other words, the shortest “distance” from the upper-left corner to the ROC curve provides the optimum set of the parameters, for which distance is given by Equation (9)<sup>8)</sup>

$$FPR = \frac{FP}{FP + TN} \quad (7)$$

$$TPR = \frac{TP}{TP + FN} \quad (8)$$

$$r = \sqrt{FPR^2 + (1 - TPR)^2} \quad (9)$$

In the parametric study for Dhunche area, the three parameters,  $i_f$ ,  $n$ , and  $i_d$ , were varied over the ranges, 35 to 45°, 0.03 to 0.3  $m^{1/3}s$ , and 10 to 30°, respectively, in an attempt to minimize the distance defined by Equation (9), and the optimum set of parameters were determined to be

$$i_f = 41^\circ$$

$$n = 0.2 \text{ m}^{1/3}s$$

$$i_d = 10^\circ$$

$$(10a), (10b), (10c)$$

with the minimum distance of  $r = 0.4989$  to the upper-left corner reached. The model correctly predicted 63 % of the observed unstable areas (TP) with an FPR of 33 %, which can include slopes that barely escaped being detached and past landslide traces.

We may also have to consider the presence of gulleys, namely cuts into steep valley walls by the erosive action of flowing water. Almost entire stretches of these gulleys are buried deeply with debris of highly weathered rock detritus. Although the earthquake occurred in the late dry season, soils and debris deposits near these cuts would certainly have been wetter than the other convex parts of the slope.

To highlight this feature of valley walls, rain concentration (RC) values<sup>9)</sup> were calculated for the entire region of the target terrain. The RC values were obtained by the following procedure:

(1) Rain particles were uniformly generated over the entire region of the target terrain in the DIPM simulation.

(2) Allowing all rain particles to be completely drained, we counted the number of rain particles that passed through each cell of the terrain grid. This number for each cell was then divided by the initial number of rain particles in one cell, and this value was defined as the RC value.

Given this reconsideration, the distance  $r$  decreases to 0.454 with  $r_t$  set at 30, and the TRP and

## 4. EVALUATION OF REMAINING

FRP values become 72 % and 35 %, respectively, when the old landslide trace is excluded. When including the old landslide trace, the distance decreases further to 0.4054 with TPR and FRP values of 73 % and 30 %, respectively.

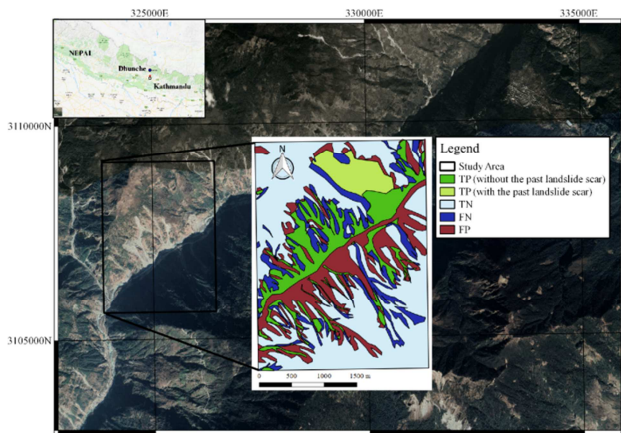


Fig. 4 Areas of landslide risk remaining (FP) in Dhunche

Not only this study but also our preliminary studies for the valley walls of the Trishuli River (Tomita, 2018<sup>10</sup>) have shown that the critical angle,  $i_f$ , is less sensitive to the location and/or extension of the target area, and fluctuate little around 40°. Assuming that the critical angle is also around 40° in Ramche, the area of remaining landslide risk is shown in Fig. 4.

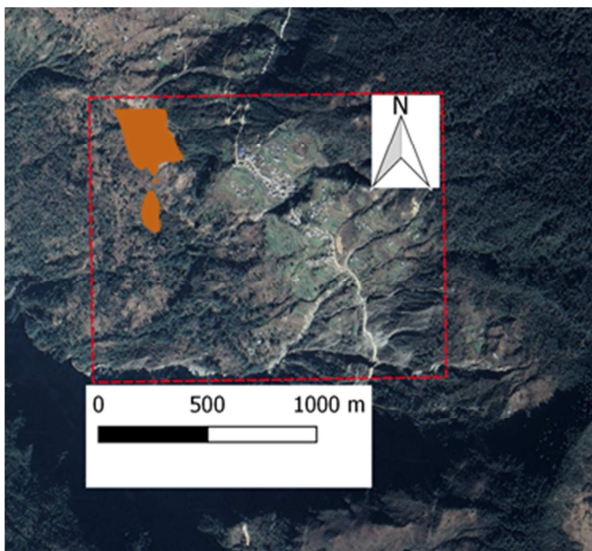


Fig. 5 Area of risk of landslide in Ramche using the numerical simulation

## 5. CREEPING MOVEMENT OF COLUVIUM DEPOSIT IN RAMCHE

A dual-frequency GPS was used to monitor the creeping movement of the colluvium deposit on a periodic basis.

The equipment used in this study is GX 1220, Leica

Geosystems. In a GPS survey, positioning accuracy is largely affected by the arrangement of four or more GPS satellites in the space. The Geometric Dilution of Precision (GDOP) is an index showing the additional multiplicative effect of navigation satellite geometry on positional measurement precision. The smaller the GDOP number, the higher is the accuracy. In this study, measurement was carried out after confirming that the GDOP at the time of measurement was 5 or less so that the error can be around 0.012m at a maximum.

In Ramche, measurements were made by Konagai et al.<sup>7</sup> in July 2015 using a series of metal pegs fixed into the ground along Ramche section of Pasang Lhamu Highway. This area was continually measured, and new pegs were also added by Tomita, et al. 2018<sup>10</sup> (Fig.5).

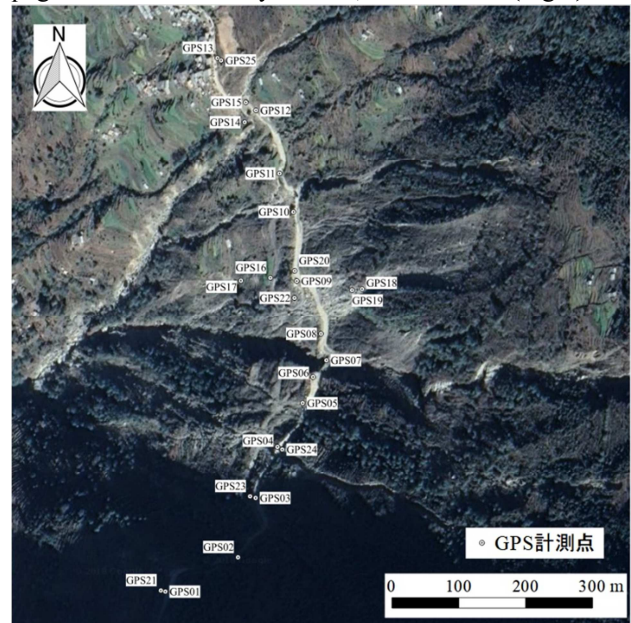


Fig. 6 GPS points location (Tomita, H., 2018)

The reference point for the survey was set to 28 ° 00 '56.31531 "N, 85 ° 12' 49.08833" E. The number of metal pegs over which we put GPS receivers went up to 25 at a maximum. However some of these pegs were occasionally lost due to rockfalls and frequent road repairs (Fig.6). The measured displacements of representative GPS points (400 times exaggerated) are shown in Fig.7 Displacements become very large in the middle of the line of metal pegs particularly near the GPS point No.20. Meanwhile displacements become very small near both ends of the line of metal pegs. The increments of displacements at these metal pegs are consistent with the cumulative displacement pattern of the highway, which has been built up over 15 years period since it was constructed in 2003.

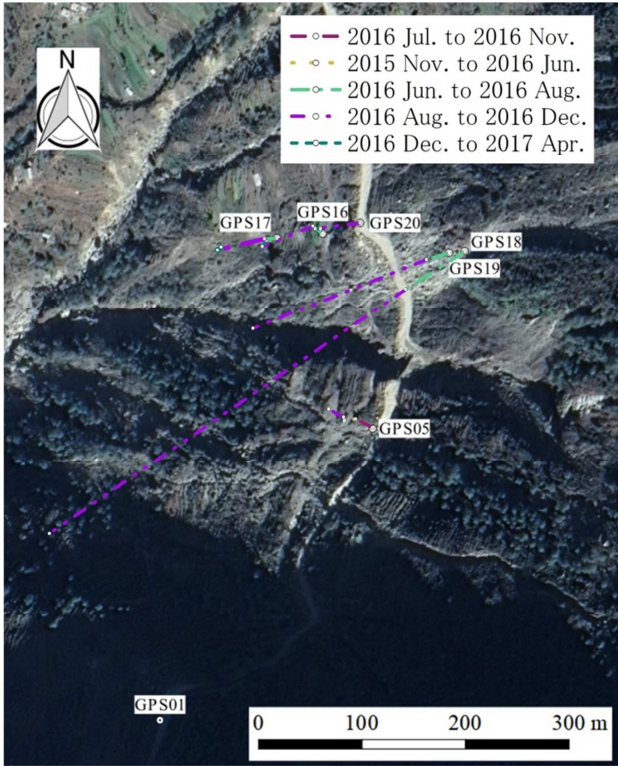


Fig. 7 Displacement of the representative GPS points (Tomita, 2018<sup>10)</sup>)

### (1) Microtremor measurements

The creeping movement of the slope can be attributed to the presence of a thick colluvium, which can be much softer than the intact bedrock underlying beneath it. If the stiffness contrast between the surface colluvium and underlying bedrock is large, ratios of spectrum amplitude of ambient ground motions to the one at the outcrop of this bedrock can indicate the presence of the colluvium.

Microtremors were recorded on September 18, 2017 using CV-374 (Tokyo-Sokushin Co. Ltd.), with the following specifications:

- Sampling frequency: 100Hz;
- Measurement range:  $\pm 0.02$  m/s ( $\pm 2$  kine);
- AD (Analog to Digital) resolution: 24 bits.

The servo-accelerometer built in the receiver is capable of recording three orthogonal components (x, y and z) of acceleration over the frequency range from 0.1 to 100 Hz. The microtremor receiver was put immediately near 5 metal pegs with its x-axis oriented along the dip direction of the slope (Fig. 8). Among these 5 points, Point MT01 is considered to be put immediately on the exposed outcrop.

The data recorded in the time domain were Fast-Fourier-transformed into the frequency

domain, and then smoothed using the Parzen Window at 0.5 Hz to obtain spectrum amplitude ratios.

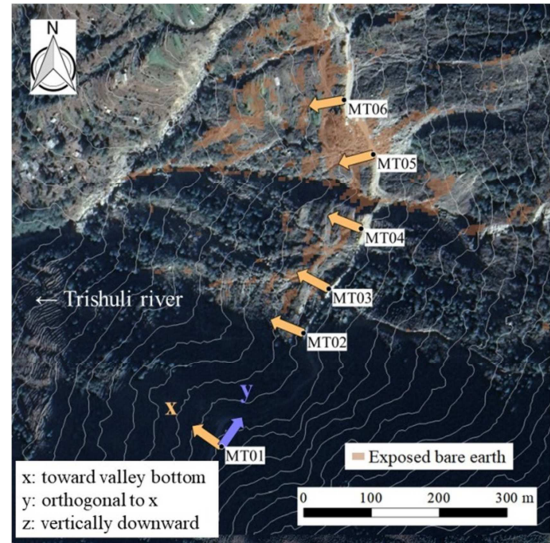
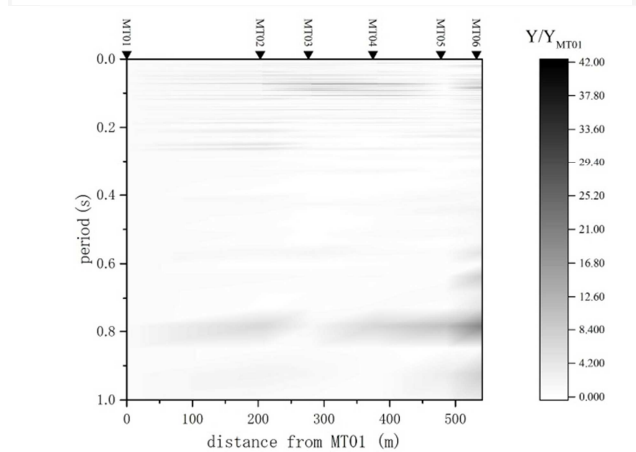
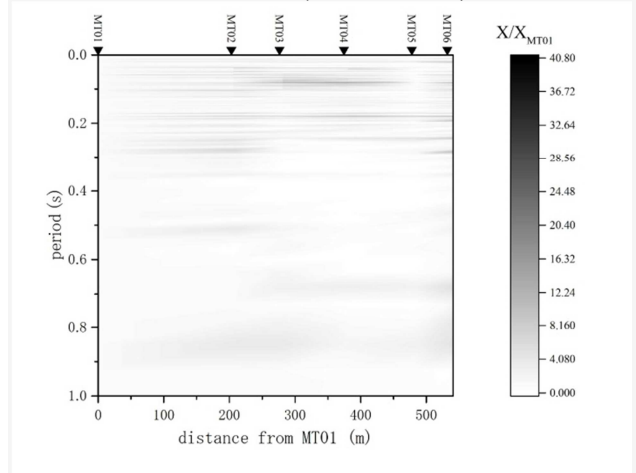
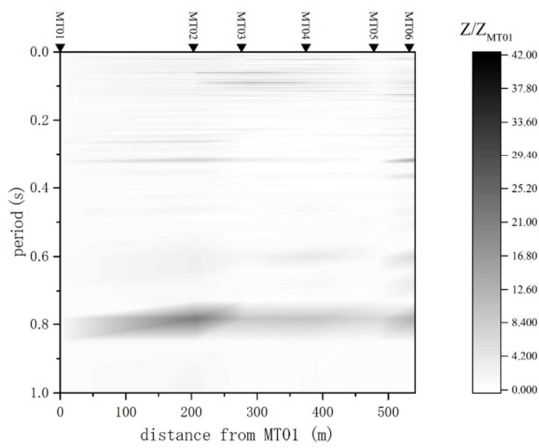


Fig. 8 Measurement points of fine movement measurement by microtremor (Tomita, 2018<sup>10)</sup>)





**Fig. 9** Spectrum results in the survey line (Tomita, 2018<sup>10</sup>)

For all components, the predominant period at which the maximum spectrum amplitude ratio is reached appears at around 0.8 s, and its fluctuation is negligibly small. Probably the entire stretch of the colluvium deposit was moving as a whole. For horizontal components, the amplitude ratio becomes larger as we get nearer to the furthest points MT05 and MT06. This may indicate that the colluvium is the thickest at around these points.

#### 4. CONCLUSION

Debris masses remaining on steep slopes in critical equilibrium with their binding forces can be detached at any time once gravity overpowers the binding strength. For the steep mountain slopes along the Trishuli River in the Himalaya struck by the 2015 Gorkha Earthquake, an attempt was made to numerically assess the remaining risk of slope failures in terms of three mechanical parameters, namely, the critical angle  $i_f$  at which a debris mass starts sliding, the Gauckler–Manning roughness coefficient  $n$ , and the angle of repose  $i_d$  for the flowing debris mass. Through a batch of numerical simulations, the optimum set of parameters was found to be  $i_f = 41^\circ$ ,  $n = 0.2 \text{ m}^{1/3}\text{s}$ , and  $i_d = 10^\circ$ , which minimized the distance to perfect classification  $r$  in the simulation to  $r = 0.4989$ . The model correctly predicted 63 % of the observed unstable areas, and the false positive rate (FPR) was 33 %.

The false positive areas included a huge past landslide mass. An up-close look at the remaining unstable slopes highlighted the presence of unstable debris masses of highly weathered and fragmented rocks accumulated along gullies. Because these materials can be wetter than materials in other areas, even in the dry season due to their being deposited

along gullies, rain concentration (RC) values were calculated for the entire region of the target terrain. The RC values were obtained by generating rain particles uniformly over the entire target terrain and by counting the number of rain particles passing through each cell of the terrain grid throughout the entire draining process. The greater part of the unstable debris mass on slopes where RC values were larger than 30 was found to have been detached during the earthquake, and the remaining debris masses with RC values close to or greater than this value could be in a state of critical equilibrium with their binding forces. The landslide positive (TP + FP) areas were thus redefined as those areas with RC values larger than 30, and the minimum distance to the perfect classification  $r$  decreased to 0.45372, with TPR and FPR values of 72 % and 35 %, respectively. When the old landslide trace was added to the TP areas, the distance  $r$  decreased further to 0.4054, with TPR and FPR values of 73 % and 30 %, respectively.

Given the difficult situation of the presence of major valley roads leading to hydropower stations and refugee camps scattered along the dry riverbed of the Trishuli, we need to keep close watch on these slopes, particularly in the FP areas.

Even slopes with their gradients less than 41 degrees may require a vigilant watch. A colluvium soil mass on a slope near Ramche about 4 to 5 km south of the target area is slowly creeping year by year. Spectrum amplitude ratios were obtained along the highway section that has been moving down inch by inch, with the southern point on the exposed bedrock as the reference. Clear predominant period at around 0.8 s may indicate the presence of the thick colluvium.

**ACKNOWLEDGMENT:** The authors are indebted to the Japan Society for the Promotion of Science, who has provided the authors with a financial support for conducting field surveys in Nepal; the support is “Detection of earthquake-induced shallow and deep-seated tectonic deformations and stresses and its implication to land conservation strategies,” Grant-in-Aid for Scientific Research (A), No. 26249069 (Leader: Kazuo Konagai). Special thanks go to Mr. Masashi Ogawa, Ambassador, Mr. Shinya Machida, Counsellor, and Mr. Makoto Oyama, First Secretary at the Embassy of Japan.

#### REFERENCES

- 1) Nakata, A. M., 2016. *Evaluation of wide-area landslide hazard using depth-integrated particle method and GIS*, Tsukuba: University of Tsukuba.
- 2) Nakata, A. M. & Matsushima, T., 2014. *Landslide*

*Simulation Based on Particle Method: Toward Statistical Risk Evaluation*. Sendai, The 1st International Conference on Computational Engineering and Science for Safety and Environmental Problems.

- 3) Nakata, A. M. & Matsushima, T., 2014. Statistical evaluation of damage area due to heavy-rain-induced landslide. *Computer Methods and Recent Advances in Geomechanics*, p. 1523–1528.
- 4) ALOS project, Advanced Land Observing Satellite, [http://www.jaxa.jp/projects/sat/alos/index\\_e.html](http://www.jaxa.jp/projects/sat/alos/index_e.html), 2011.
- 5) Bui, H. H., Fukagawa, R., Sako, K. & Ohno, S., 2008. Lagrangian meshfree particles method (SPH) for large deformation and failure flows of geomaterial using elastic–plastic soil constitutive model. *Numerical and analytical methods in geomechanics*, 32(12), pp. 1537-1570.
- 6) Paz, M. R. & Bonet, J., 2005. A corrected smooth particle hydrodynamics formulation of the shallow-water equations. *Computers & Structures*, 83(17-18), pp. 1396-1410.
- 7) Konagai, K., et al., *Follow-up report of damage caused by the Gorkha Earthquake, Nepal, of April 25 th, 2015*. FS 2016-E-0002: JSCE Journal of Disaster FactSheets, 2016 ..
- 8) Cepeda, J. M., Nadim, F. & Hoeg, K., 2010. Landslide-triggering rainfall thresholds: A conceptual framework. *Q J ENG GEOL HYDROGEOL*, 43(1), pp. 69-84.
- 9) Nakata, A. M. et al., 2017. *Analysis of landslides effects triggered by Gorkha Earthquake along Trishuli River*. Kumamoto, JSCE Symposium on Earthquake Engineering.
- 10) Tomita, H., 2018, xxxx master thesis, Yokohama National University.
- 11) Saeki, Y., Morihei, I., Kono, K., Kano, K.,. *Amplification characteristics of highway embankment by microtremoring at all times* p.1785-1786: Lecture of the 42nd Earthquake Engineering Research Presentation, 2007 (in Japanese).
- 12) Izumi, S., Ohara, .., *Estimation using vibrational behavior of steep slope slope with constant microtremor*. Proceedings of the 25th Earthquake Engineering Research Presentation Paper: p.229-232, 1999 (in Japanese).

**(Received August, 2018)**